Mass Discrimination Effects in an Ion Detector and Other Causes for Shifts in Polymer Mass Distributions Measured by Matrix-Assisted Laser Desorption/Ionization Time-of-Flight Mass Spectrometry

Jan Axelsson,* Elaine Scrivener, David M. Haddleton, and Peter J. Derrick

Institute of Mass Spectrometry and Department of Chemistry, University of Warwick, Coventry CV4 7AL, United Kingdom

Received March 5, 1996; Revised Manuscript Received August 13, 1996[⊗]

ABSTRACT: Recent attempts to employ matrix-assisted laser desorption/ionization time-of-flight mass spectrometry for polymer characterization have claimed successful matches with more traditional methods such as size exclusion chromatography. In this paper, we describe how the resulting molecular mass distribution is not only extremely sensitive to ionization conditions such as laser power but also sensitive to the mass- and velocity-dependent detector system. For a broad polymer distribution (polydispersity > 2), employing similar ionization conditions and varying only the kinetic energy with which an ion impinges onto a detector surface, the mass corresponding to the most probable peak can be significantly shifted. Differences in shape of the measured distribution and the shift in the most probable peak are explicable by existing theories for secondary electron emission. We propose a criterion for selecting the ion kinetic energy in order to minimize spectrum distortion.

Introduction

Determination of accurate relative molecular masses of synthetic polymers is often difficult to achieve. Detailed information on molecular structure, such as identification of end groups and location of branching points, can be even more elusive. Burgeoning developments in polymer design and synthesis are creating ever more complicated macromolecular structures for specific applications. Size exclusion chromatography (SEC) is usually a relative method relying on calibration with polymers of known molecular masses. However, extremely limited narrow molecular weight standards are available and most SEC is quoted relative to polystyrene. This is an obvious limitation as there are many different hetero- and copolymers. SEC traces are usually broad envelopes at all but the lowest mass (usually <500 Da) and devoid of information regarding individual molecular species. Thus, the level of detail regarding macromolecular structure is not available by SEC. A technique finding increasing application and popularity for polymer mass analysis is matrix-assisted laser desorption/ionization (MALDI) time-of-flight (TOF) mass spectrometry (MS).

The most common type of detector employed in TOF mass spectrometry of large molecules relies either on direct ion-to-electron conversion (predominant at velocities above ≈20−30 km/s) or, for lower velocities, on primary-ion to secondary-ion conversion followed by ion-to-electron conversion. The conversion takes place either at the detector surface itself or at a conversion dynode. The electron signal produced is subsequently amplified in an electron multiplier, and the resulting charge is collected. Two singly charged ions of different masses which are accelerated through the same potential difference will have different velocities at the detector surface. Since the number of emitted secondary electrons is a function of the incident ion mass and velocity, such ions of different masses will generally cause different numbers of secondary electrons to be emitted at the detector surface. Two ions of different masses will hence yield different signal amplitudes from the detector. The question to be addressed is whether the magnitudes of such differences are likely to be sufficiently large to be significant in the context of TOF mass spectrometry of polymers.

MALDI-MS[1,2] is not generally applicable as a quantitative method. Attempts have been made to show that MALDI-MS may be used for quantitative measurements using internal calibrants which are similar to the analyte in mass and chemical composition,[3,4] thus utilizing the expected similarities in ionization probability. The normally uncontrolled ionization efficiency has caused biomolecular mass spectrometrists to use MALDI-MS cautiously, generally employing it as a tool for deducing the masses but *not* for calculating sample concentration or even relative concentrations from measured intensities.

For polymer analysis, however, it has been assumed that different oligomers display equal ionization probability.[5−13] Results have been published for poly(methyl methacrylate) (PMMA), polystyrene, poly(ethylene glycol), and poly(butyl methacrylate) for which MALDI-MS and SEC agree.[5−13] Results have also been published for poly(butyl methacrylate) and PMMA for which the number-average molecular masses (M_n) have disagreed.[12,14] It seems to be a common phenomenon that disagreement between MALDI-MS and SEC occurs for high polydispersities (broad polymer mass distributions).[12,14] However, even an apparent agreement between MALDI-MS and SEC for narrow molecular mass PMMA and polystyrene mass distributions has been reported to exhibit systematic errors, indicating a preference to observe components of slightly lower mass preferentially.[5] This results in M_w (mass-average molecular mass) being lowered to a greater extent than M_n, thus resulting in not only a measured M_w being too low but a measured molecular mass distribution appearing narrower than its true value.

* Corresponding author.

[⊗] Abstract published in *Advance ACS Abstracts,* November 15, 1996.

S0024-9297(96)00350-6 CCC: $12.00

We are of the opinion that, for *wide* polymer distributions ($M_w/M_n > 2$), agreements between MALDI-MS spectra without any correction and SEC are fortuitous, probably reflecting the fact that not enough effort has been made to choose the laser power correctly. Ideally, the laser power should be chosen so that the ionization probability is the same for all ions, but simultaneously, so that the laser power is not so high as to cause fragmentation. Even if identical ionization probabilities have been achieved, effects such as the detector response may affect the measured polymer mass distribution significantly, depending upon the characteristics of the detector. This effect can be minimized by choosing the acceleration voltage carefully or can be corrected for if the response function of the particular detector employed is known.

In this paper, we will show that due to the different detector response to ions of different masses the position of the most abundant peak of even a low-mass polymer distribution can be shifted by several hundred mass units, corresponding to several repeat units. We will also show the importance of selecting a correct acceleration voltage, so that the shift can be minimized, as well as exemplifying other reasons such as ionization effects and ion optical effects which can shift the most abundant peak both up and down in the spectrum. All of these results concern a Kompact MALDI III instrument (see Experimental Section); the characteristics of other instruments will differ quantitatively but not qualitatively.

Experimental Section

Mass Spectrometry. A Kratos Kompact MALDI III (Kratos Analytical Ltd., Manchester, UK) time-of-flight (TOF) mass spectrometer was employed in its reflectron mode of operation. Both 5 kV ("low-mass" mode) and 20 kV ("high-mass" mode) extraction potentials were employed. The instrument is equipped with a 337 nm nitrogen laser with a pulse duration of 3 ns. As supplied by the manufacturer, the laser beam is attenuated by a neutral-density filter which gives a logarithmic power scale. All of our measures of power are quoted on a linear scale. For the 20 kV extraction potential, the data were averaged over 20−50 laser shots, and for the 5 kV extraction potential, data were averaged over 100−500 shots. The laser beam was scanned along a line over the 2 mm sample spot to minimize sample deterioration.

The instrument employs an ETP time-of-flight electron multiplier with an ion-to-electron converting Al_2O_3 dynode surface placed perpendicular to the ion flight path (ETP, Sydney, Australia). In this instrument the dynode surface is grounded[15] so that the *extraction voltage V* in the ion source equals the *total acceleration voltage U* through which the ions are accelerated from sample to detector surface.

Polymer Preparation and Characterization. Size exclusion chromatography (SEC) was carried out on a Polymer Laboratories modular SEC system. The elutant was THF at 1 cm^3/min with calibration against 12 narrow PMMA molecular mass standards of 200 to 1 100 000 Da. Data manipulation was carried out using PL Caliber Software, and number distributions were calculated using a standard spreadsheet program.

Two samples of poly(methyl methacrylate) (PMMA) were synthesized by catalytic chain transfer polymerization.[16] The PMMA samples were characterized by SEC as having number-average masses $M_n = 1520$ and $M_n = 2998$, mass-average molecular masses $M_w = 3131$ and $M_w = 4796$, and polydispersities $PD_i = 2.06$ and $PD_i = 1.60$. Catalytic chain transfer polymerization results in PMMA having the structure shown in Figure 1, with residual masses of $100.12 \times (x + 1)$.

Poly(ethylene glycol) (PEG) supplied as having average mass $M_n = 1400-1600$ Da was obtained from Fluka Chemicals, Gillingham, Dorset, England (Figure 1). For sake of completeness, we also characterized this sample by SEC using a PMMA calibration standard.[17]

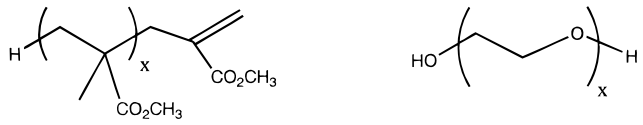

PMMA PEG

Figure 1. Structurea of (a) PMMA and (b) PEG. The *x* repetitive units are drawn within parentheses.

MALDI Sample Preparation. For MALDI-MS, 20 sample spots were prepared on a stainless steel slide employing the following procedure. (1a) *For PMMA*: 5 parts of a solution of 0.1 M 2,5-dihydroxybenzoic acid in acetone was mixed with 1 part of deionized water. A 0.5 μL drop of this mixture was deposited onto each sample spot. (1b) *For PEG*: 0.1 M of 2,5-dihydroxybenzoic acid was dissolved in a 9:1 water:ethanol mixture, of which a 0.5 μL drop was deposited onto each sample spot. (2) The samples were then dried for 5 min at room temperature under a flow of air. (3a) *For PMMA*: 5 parts of 10^{-3} M PMMA in acetone, mixed with 1 part of deionized water, was then dropped on top of the dried matrix. (3b) *For PEG*: a 10^{-3} M aqueous solution of PEG was dropped onto the dried matrix. (4) The samples were again air-dried for 5 min (as in point 2).

Analysis. The ion flight times in the Kratos Kompact III instrument are recorded with a digital storage oscilloscope by sampling a voltage which corresponds to the charge deposited on the detector anode. This voltage is sampled every 3.3 ns, so that the sample rate is high enough not to limit the resolution of the spectrometer. Therefore, ions of the same mass-to-charge ratio will generally be recorded in several adjacent channels. Because the time-of-flight technique involves a nonlinear transformation between time scale and mass scale, peak heights at different masses will be unequally weighted.

The intensities of all channels within a spectral peak have to be summed (thus obtaining the peak areas in the time domain), and this has to be repeated for each peak. The peak areas are then plotted in a bar graph, where each peak area is represented by the height of a bar, thus transforming a peak-height spectrum to a (peak area) number distribution spectrum.

Results and Discussion

Reproducibility and Sample Decay. MALDI matrices can exhibit poor homogeneity, resulting in poor spot-to-spot reproducibility. For instance, the most intense signal when the DHB matrix is used[18] is often obtained from the sample edges. However, in our experiment the signal intensity profile along the sample was reproducible, so that spectra averaged along the same portion of the sample at different scans could be reproduced. Normally, between 20 and 50% of the shots in a scan gave useful information.

Sample exposure effects have been reported, in which the peak shape in a MALDI mass spectrum varies with the number of laser shots.[19] We were therefore concerned that the shape of a polymer distribution might exhibit similar sample exposure effects.

The laser spot size was measured by ablation of blue ink and found to be approximately 60 μm wide and 500 μm long, tilted approximately 30° away from the scanning axis. This means that the smallest distance the laser spot can be shifted without overlapping the previous shot is approximately 70 μm. Scanning the laser uniformly over the 2 mm sample therefore ensured that each spot on the sample on average only received approximately 1/30th of the total number of shots employed in a scan. On scanning the laser twice over the same PMMA 1520 sample firing 50 shots per scan,

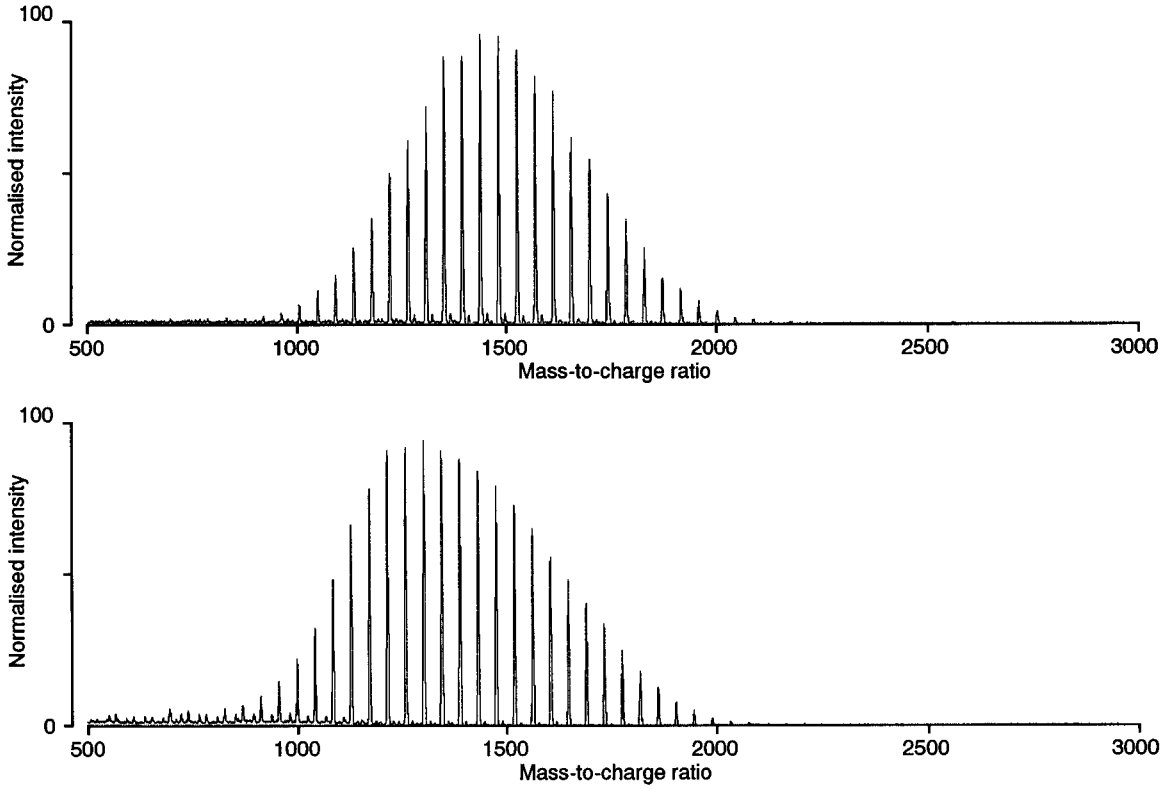

Figure 2. Top, the symmetric MALDI mass spectrum of PEG 1500 acquired with a laser power $1.3\phi_{th}$ (ϕ_{th} = threshold power). Bottom, the same sample acquired with a laser power $1.7\phi_{th}$. The higher power favors lower mass peaks as seen in the skewing of the distribution in the lower spectrum.

two virtually identical spectra were acquired (results not shown). However, after a large number of shots, the measured distributions generally became less smooth, so that the shapes of two distributions could not be directly compared.

In a second experiment, with the scanning laser, a total of 600 shots were fired onto a sample of PMMA 1520. After several hundred shots, the low-intensity peaks at high masses (above ≈3500 Da) could not be distinguished from the noise. To probe for changes in the shape of the measured distributions we therefore calculated M_n using peaks between 600 and 3500 Da, each spectrum averaged over 100 shots. For the first 500 shots, M_n fluctuated between 1911 and 1980 Da.

The results from these two experiments indicate that for the first 500 shots the sample deterioration caused by laser ablation did not significantly alter the shape of the polymer mass distributions. Therefore, the number of laser shots per sample was kept below 500 for all experiments reported.

Laser Power Effects on Distribution. A careful choice of the laser power is extremely important for spectral quality in MALDI. There is an obvious trade-off between obtaining enough intensity (high laser power) and obtaining a spectrum without signs of fragmentation or distortions (low laser power). For PEG 1500, PMMA 1520, and PMMA 2998, we normally employed a power of 1.3 times the threshold power ($1.3\phi_{th}$), on a linear power scale. The neutral-density filter on our Kompact III gave a laser power proportional to $10^{(0.0106S-2.0)}$, with S being the power setting on the instrument.[15] The threshold power ϕ_{th} was defined as the extrapolated (linearized) power at which the total peak area of the polymer distribution became zero.

We used power settings $S = 125$ for PEG and $S = 135$ for PMMA 1520 and PMMA 2998. For some samples, however, we occasionally found that higher power was needed to get a high-quality spectrum, and consistently on these samples the power required to obtain a given degree of fragmentation was higher than normal.

We found that for power $S = 125$ ($1.3\phi_{th}$) the PEG 1500 displayed a symmetric Gaussian-like distribution. However, after increasing the power to $1.7\phi_{th}$, the distribution was significantly skewed toward lower mass (Figure 2).

For PMMA 2998, increasing the laser power from $1.3\phi_{th}$ to $1.6\phi_{th}$ resulted in a second distribution appearing at approximately twice the mass. This could possibly be explained as dimerization taking place in the gas phase, similar to reported gas-phase clustering of small biomolecules in supersonic beam expansion.[20] This effect was observed in linear time-of-flight mode (Figure 3), which has also been reported by others.[12,21,30] Similar nonspecific clustering of proteins has recently been reported for linear time-of-flight MALDI.[22] A possible explanation to why we do not see the distribution at twice the mass in the reflectron mode is that dimerized ions are metastable and that the dimers decay into one neutral and one singly charged ion before the ion mirror (reflectron).

In reflectron mode we observed that an increase in power from $1.3\phi_{th}$ to $1.6\phi_{th}$ resulted in the distribution widening (data not shown). This could be explained by a combination of increased dimerization intensifying higher mass peaks and a skewing of the distribution (compare with PEG in Figure 2). A shift in the position of the most probable peak toward higher masses was also observed. The signal to noise ratio is also affected by laser power. When the laser power was too low, the sensitivity was not high enough to measure peak areas of low-intensity peaks (often high-mass peaks) from the noise, and therefore measured mass averages were irreproducible.

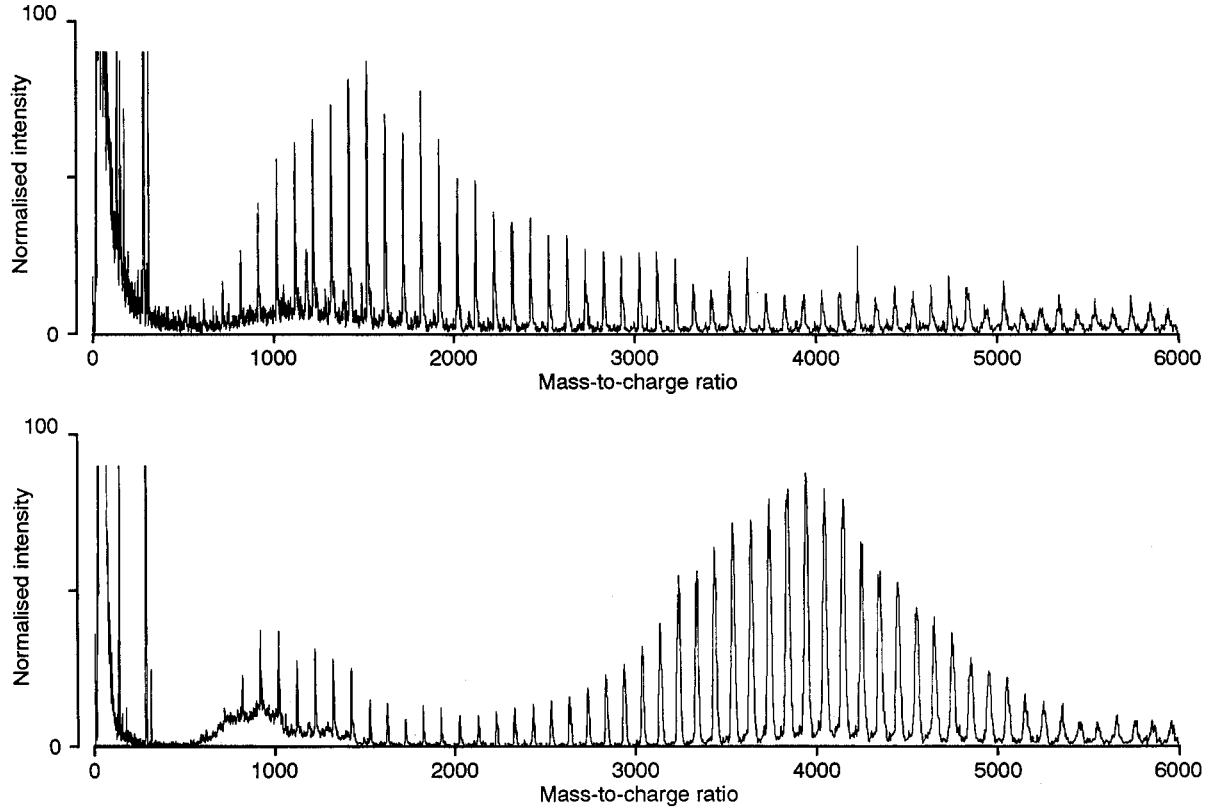

Figure 3. PMMA 2998 spectra at relatively high power acquired in linear time-of-flight. The top spectrum was acquired at a power of $1.3\phi_{th}$, and the bottom spectrum at a power of $1.6\phi_{th}$. A second distribution appears at approximately twice the mass of what is expected from a PMMA 2998 mass spectrum.

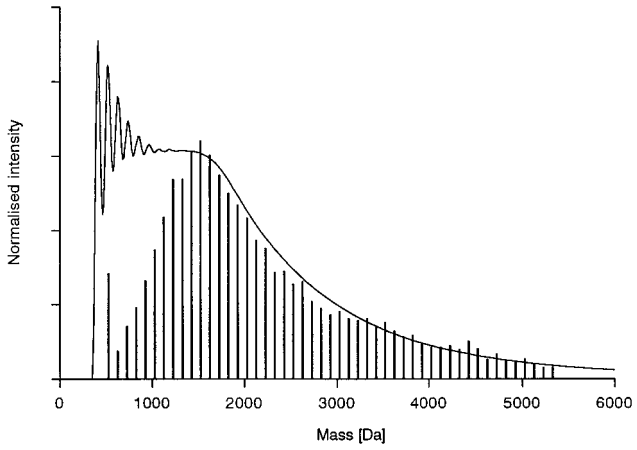

Figure 4. Discrimination of low-mass oligomers of PMMA in MALDI illustrated by comparison of the PMMA 1520 number distribution from SEC (line plot) and MALDI-MS at 20 kV acceleration potential (bars). The height of a bar equals the area of the corresponding MALDI-MS peak.

Other Ionization Effects. Comparing a number mass distribution calculated from a SEC spectrum to a number distribution spectrum from a PMMA 1520 MALDI-MS spectrum acquired at 20 kV extraction voltage, it is obvious that compared to SEC, MALDI-MS was discriminating against the low-mass ions (Figure 4). Work is in progress to further elucidate this effect.

Ion Optical Effects. Ions are produced with initial velocities distributed both axially and radially.[23−25] The axial velocity component is small relative to the velocity obtained from the extracting voltage in the MALDI source. The radial component, however, is in a first approximation conserved throughout the flight path of the Kompact MALDI III, leading to a cone of ions displaced from the central axis of the instrument. The radius of this cone equals

$$r = v_r t = v_r \frac{L}{(2eZV/M)^{1/2}} \quad (1)$$

with initial velocity v_r [m/s], length of flight path L [m], ion mass M [kg], ion charge eZ [C], and extraction voltage V [V]. Equation 1 shows that in a mass spectrometer (constant extraction voltage and flight length) the radius is approximately proportional to the square root of mass, assuming small variations in radial velocity with mass. A radial velocity (at 50% of maximum intensity) of 280 m/s (2.4 eV) was measured for insulin in sinapinic acid.[23] For a matrix of α-cyano-4-hydroxycinnamic acid, radial velocities have been determined to 381 m/s for insulin and 390−470 m/s for luteinizing hormone releasing hormone (LHRH).[25] The maximum radial velocity of substance P in a DHB matrix can, from ref 24, be approximated to 580 m/s.

For the Kompact MALDI III instrument length of 0.7 m, the radial divergence in linear mode can for insulin be calculated to between 14 and 20 mm for a 5 kV extraction voltage and between 7 and 10 mm for a 20 kV extraction voltage. The corresponding divergence radii in reflectron mode are approximately twice these calculated for the linear mode. Comparing a typical electron multiplier detector radius of ≈5 mm with the 40 mm divergence radius for 5 keV insulin ions in reflectron mode, we conclude that only the core of the beam will hit the detector. The intensity distribution of the desorbed ions is proportional to $\cos^{2.39}(\alpha)$,[26] a function which is approximately flat for small initial desorption angles α. The limited part of the beam profile of desorbed ions incident onto the active area of the detector corresponds to small angles α when the

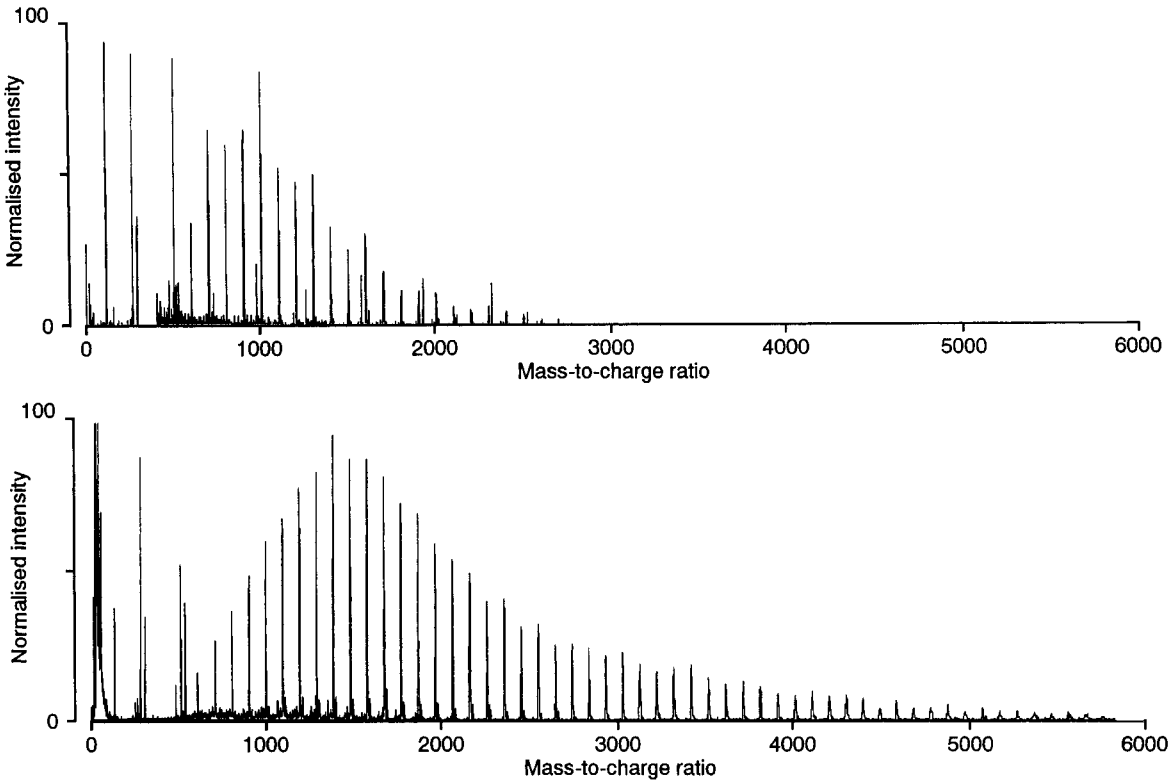

Figure 5. The distinctly different spectra of PMMA 1520 acquired at 5 kV acceleration voltage (top) and 20 kV acceleration voltage (bottom).

divergence radius r is larger than approximately 3 times the detector radius r_d. If $r > 3r_d$ for the lightest mass of interest, then $r > 3r_d$ for all heavier masses. Discarding the ions for which $r > 3r_d$, the resulting beam profile can be approximated by a flat intensity distribution. For the flat beam profile, the resulting fraction of desorbed ions which will hit the active area of the detector πr_d^2 is

$$\frac{\pi r_d^2}{\pi r^2} = r_d^2 \frac{e}{L^2} \frac{V}{M/Z} \frac{1}{v_r^2} \tag{2}$$

which will induce a skewing of a polymer distribution even before taking the detection efficiency into account. This skewing due to ion optics could be avoided by ensuring that all desorbed ions impact the active area of the detector. This requires either a large (expensive) detector or focusing of the ions, which may decrease the resolution of the instrument.

Interestingly, the skewing of two polymer distributions due to this ion optical effect is approximately independent of extraction voltage and flight length (as long as the divergence radius is more than about 3 times that of the detector radius). That to say, employing eq 2, the fraction of ions of mass M_1 hitting the detector divided by the fraction of ions of mass M_2 hitting the detector is independent of V and L. Hence, large differences in mass spectra measured at different extraction voltages (as in Figure 5) can not be explained by this ion optical effect.

Detector Effects. Acquiring two spectra using different extraction potentials but the same sample and the same laser power gave two distinctly different polymer distributions (Figure 5). This could be thought of as being a result of different extraction electric fields. However, as has been reported in ref 27, employing delayed extraction, (relative-intensity) polymer envelopes are identical for different delay times. This would suggest that collisions between polymer ions and the plume of the matrix have similar consequence for all oligomers in the polymer distribution, regardless of the plume density at the time when the electric field is applied. A higher plume density means that the ion mean free path is decreased and, therefore, that collisions between ions and matrix molecules become more frequent and therefore less energetic. With a relatively high extraction field applied at zero delay time, the collisions become more energetic than for a low field. We believe that the differences between the spectra acquired at 5 and 20 kV extraction potentials cannot be attributed to differences in extraction fields, and we will proceed to investigate whether the change in a distribution can be explained by the mass and velocity dependence of the detector signal.

The detector signal is a linear function of the charge collected by the electron multiplier anode, which in turn for this electron multiplier configuration is a linear function of the number of initial secondary electrons produced from the ion-to-electron conversion. For ion velocities below approximately 30 km/s, few secondary electrons are created and the average number of secondary electrons γ from singly charged biomolecules incident on a semi-conducting surface of a microchannel plate detector is described by the empirical formula[28]

$$\gamma_L = am\, e^{bv} \tag{3}$$

Here, v is the ion velocity [m/s], m is the ion mass in atomic mass units [Da], and the parameters for that particular microchannel plate detector were reported to be $a = 2.58 \times 10^{-7}$ and $b = 2.31 \times 10^{-4}$.[28]

Similarly for velocities above about 30 km/s, the number of secondary electrons from large multiply

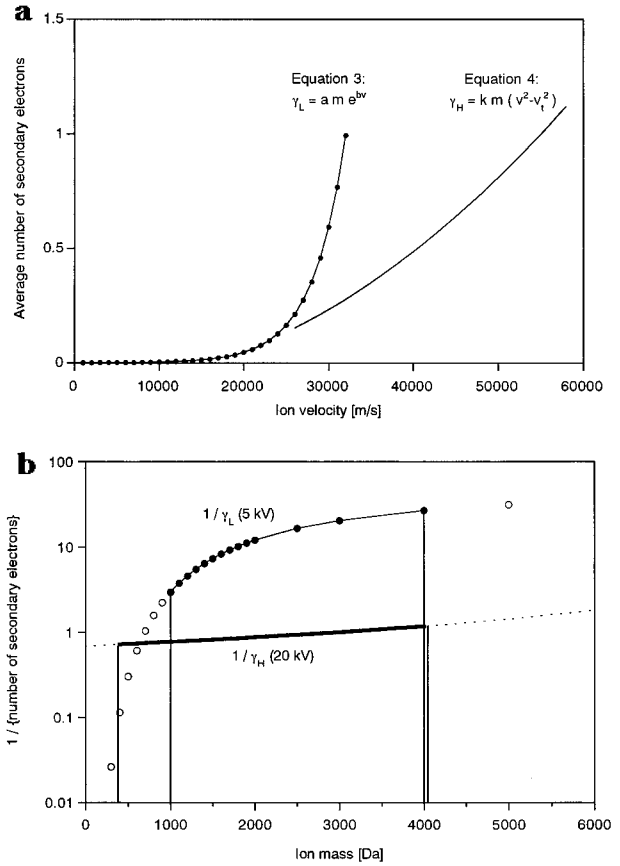

Figure 6. (a) Number of secondary electrons emitted in the detector per incident ion (eqs 3 and 4) plotted as a function of ion velocity. Equation 3 is valid below 25−30 km/s, and eq 4 is valid at velocities between approximately 30 and 100 km/s. (b) The inverse of the number of secondary electrons equals the correction function with which a measured distribution should be multiplied by in order to correct for distortions introduced by the detector response. The valid ranges for eqs 6 (filled circles) and 7 (solid line) are indicated in the figure.

charged biomolecules incident on graphite can be described by

$$\gamma_H = km\,(v^2 - v_t^2) \tag{4}$$

where the proportionality constant k is target dependent, and the extrapolated threshold velocity is of the order of 25 km/s.[29]

The secondary electron yield as described by the two formulas (3) and (4) is plotted in Figure 6a, and it is obvious that the dependence in (3) is increasing too sharply for velocities above 30 km/s. The two dependences (3) and (4) are only valid over their specified ranges.

For MALDI-MS of singly charged ions, all the ions are accelerated from the sample to the detector surface over the same total acceleration voltage U [V]. Note that for our experiments, the extraction voltage and the total acceleration voltage onto the detector surface are the same. The velocity of a particular singly charged ion is thus a function of the ion mass M in kilograms, which can be described by

$$v = \left(\frac{2eU}{M}\right)^{1/2} = 13.9 \times 10^3 \left(\frac{U}{m}\right)^{1/2} \tag{5}$$

where in the second expression in (5) the ion mass m is expressed in daltons. Inserting (5) into (3) and (4) respectively, the secondary electron yield for velocities below approximately 30 km/s can be described by

$$\gamma_L = am\ e^{B(U/m)^{1/2}} \tag{6}$$

and the yield for velocities above approximately 30 km/s may be described by

$$\gamma_H = km[(13.9 \times 10^3)^2\,(U/m) - v_t^2] = k[CU - Dm] \tag{7}$$

Equations 6 and 7 describe the number of secondary electrons emitted (at the ion-to-electron conversion in the detector) as a function of ion mass. As follows from the introduction, this means that these equations can also be interpreted to describe the ion signal as a function of mass; i.e. the measured intensity for any mass is proportional to the secondary electron yield and to the number of incident ions.

In order to calculate a mass-independent ion intensity spectrum, a correction function which is proportional to $1/\gamma$ has to be applied to the measured spectrum. The correction functions $1/\gamma_L$ (for 5 kV extraction voltage) and $1/\gamma_H$ (20 kV) are plotted in Figure 6b. As may be calculated from (5), $1/\gamma_L$ is valid over the approximate range 1000 Da (v = 30 km/s) to 4000 Da (v = 15 km/s) for U = 5000 V, and $1/\gamma_H$ is valid from about 400 Da (v = 100 km/s) to 4000 Da (30 km/s) for U = 20 000 V. The two functions overlap in the very parts of the mass range which are relevant to the polymer distributions used in these experiments. Therefore, once the parameters in the correction functions are determined, we can correct the widely different mass spectra which are acquired at different extraction potentials. Ideally, these corrected spectra should be identical.

The parameters for formulas 6 and 7 were obtained by the following method: The 5 kV number distribution spectrum $I_5(m)$ was divided by the 20 kV number distribution spectrum $I_{20}(m)$, and the resulting $I_5(m)/I_{20}(m)$ was compared with $\gamma_L(m)/\gamma_H(m)$. The parameters were adjusted so that the statistical χ^2 was minimized. The parameter values for eqs 6 and 7 are $B = 3.59$, $C = 1.93 \times 10^8$, and $D = 2.56 \times 10^8$, which gives the values $a/k = 7.2 \times 10^5$, $b = 2.58 \times 10^{-4}$, and $v_t = 1.6 \times 10^4$ for the parameters in (3) and (4). The fraction a/k is an instrument-dependent normalization constant whose value is uninteresting with respect to correcting the shape of a measured spectrum. Noteworthy, the value $b = 2.58 \times 10^{-4}$ compares well to the reported value 2.31×10^{-4}.[28] The value of the extrapolated threshold velocity v_t is somewhat lower than the expected ≈23 km/s.[29] The threshold velocity could however be fixed to 23 km/s without significantly altering the goodness of the χ^2 fit. This implies that formulas 6 and 7 become uncertain at velocities very close to the threshold velocity.

Correcting Spectra for Detector Effects. The correction functions $1/\gamma_L$ and $1/\gamma_H$ can now be employed to correct spectra which are measured at badly chosen extraction voltages. One test is the PMMA 1520 spectrum acquired at a 5 kV extraction potential, which is significantly different from the spectrum acquired at a 20 kV potential. Figure 7 shows how the most probable mass M_p (defined as the most intense peak) of the PMMA 1520 number distribution spectrum measured at 5 kV is shifted by 468 Da from M_p = 1024 Da to M_p = 1492 Da after multiplication by the correction function $1/\gamma_L$. The latter value is the maximum of the continuous envelope drawn through the corrected mass spectrum (Figure 7, top, open circles) and does not

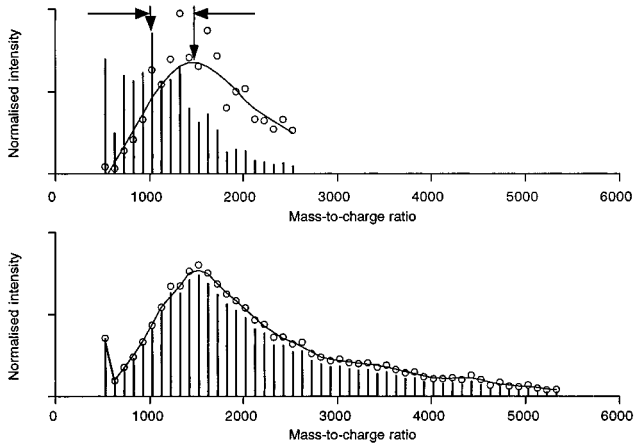

Figure 7. Measured (bar graph) and corrected (line) PMMA 1520 number distribution spectra for 5 kV (top) and 20 kV (bottom) acceleration voltages. The measured and the corrected spectra for 20 kV are almost identical. This suggests that a 20 kV voltage acceleration voltage is preferable for ions in a mass window similar to the PMMA 1520 distribution.

correspond to a mass calculated from the PMMA 100.12 $\times$ (x + 1) + Na formula. Multiplying the PMMA 1520 number distribution spectrum acquired at 20 kV by $1/\gamma_H$ induces a shift of only 26 Da (compared to 468 Da for 5 kV).

This difference is easily explained by examining Figure 6b for the mass window from 1000 to 4000 Da. For 20 kV the correction function $1/\gamma_H$ only increases 1.5 times whereas for 5 kV the correction function $1/\gamma_L$ increases 9 times. A much larger distortion of the polymer distribution is therefore expected in the spectrum acquired at 5 kV. A much smaller distortion of the mass spectrum occurs when the extraction voltage is chosen so that the ion mass is within the quadratic region of the secondary electron yield (in this case, 20 kV) than when the ion mass is within the exponential electron yield region (for this ion, 5 kV). In the quadratic region, for velocities much larger than the threshold velocity the secondary electron yield is proportional to ion kinetic energy eZU, thus independent of mass and only depending on ion charge Z. Hence for these high velocities, in theory no correction is necessary. For lower velocities however, the ions of interest should exhibit velocities (eq 5) above approximately 30 $\times$ 10^3 m/s to minimize distortion. In Figure 8, the singly charged ion velocities are plotted as a function of total acceleration voltage (from MALDI sample spot to detector surface) with mass as parameter. For a given mass, Figure 8 thus supplies an estimate of the minimum acceleration voltage required for the ion velocity to exceed 30 km/s.

Similarly (data not shown) examining PEG 1500 distributions acquired at 5 and 20 kV, we found a 38 Da shift from the measured to the corrected distribution for 5 kV extraction potential, but only a 3 Da shift for the 20 kV potential. The small shifts were due to the narrowness of the PEG 1500 mass distribution.

That narrow mass distribution polymers give a rather accurate measurement of both M_p and M_w even at unfavorable extraction potentials explains observations where[5] MALDI mass spectra of PMMA faithfully reproduced M_p and M_w obtained by SEC.

Conclusions

We note that low-mass oligomers display ionization properties different from higher mass oligomers. Because of this, MALDI-MS cannot be expected to measure accurately number distributions which include low-mass oligomers. We also demonstrate that effects such as laser power and ion optical mass discrimination effects can skew a measured polymer mass distribution significantly in the Kompact MALDI III.

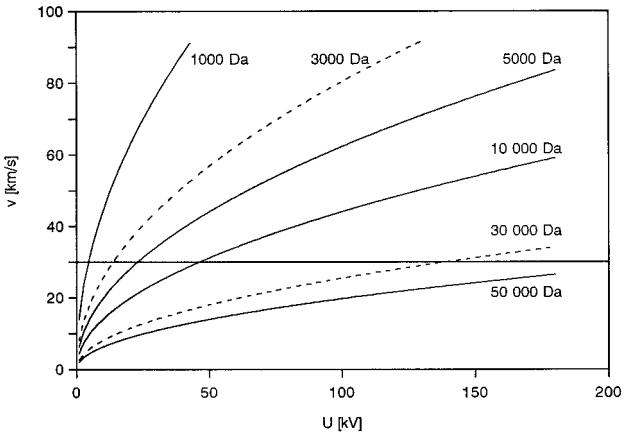

Figure 8. Singly charged ion velocities plotted as a function of total acceleration voltage into the detector surface. The voltage required for the ion velocity to exceed 30 km/s (horizontal line) can be estimated, which can serve as guideline for selecting total accelerating voltage.

The significant changes in the shape of the polymer mass spectrum have been fully explained on the basis of the predicted mass and velocity dependence of the secondary electron emission from the detector surface. We show that the spectra measured on the Kompact MALDI III can be corrected by applying a correction function based on the mass and velocity dependence of the secondary electron emission. To minimize distortions due to the detector response, we propose that the potential difference between ion formation and ion detection be chosen so that the ion velocity at the detector exceeds approximately 30 km/s for the mass window of interest. The mass at which this minimum velocity occurs is directly proportional to the voltage between sample and detector surface, and hence different mass spectrometers are likely to display mass discrimination effects starting at different masses. Once these problems with mass spectrometry of polymers are resolved, MALDI TOF promises to provide a greater level of detail without the calibration problems encountered in size exclusion chromatography.

Acknowledgment. We are grateful for financial support from the European Network on Biomolecular Mass Spectrometry (ENBHS) and from the Engineering and Physical Sciences Research Council (Grant GR/H94504). We wish to thank D. R. Maloney for preparation of the PMMA samples used in this study.

References and Notes

(1) Karas, M.; Hillenkamp, F. *Anal. Chem.* **1988**, *60*, 2299.
(2) Hillenkamp, F.; Karas, M.; Beavis, R. C.; Chait, B. T. *Anal. Chem.* **1991**, *63*, 1193A.
(3) Duncan, M. W.; Matanovic, G.; Cerpa-Poljak, A. *Rapid Commun. Mass Spectrom.* **1993**, *7*, 1090−1094.
(4) Jespersen, S.; Niessen, W. M. A.; Tjaden, U. R.; van der Greef, J. *J. Mass Spectrom.*, **1995**, *30*, 357−364.
(5) Lloyd, P. M.; Suddaby, K. G.; Varney, J. E.; Scrivener, E.; Derrick, P. J.; Haddleton, D. M. *Eur. Mass Spectrom.* **1995**, *1*, 293−300.
(6) Danis, P. O.; Karr, D. E.; Mayer, F.; Holle, A.; Watson, C. H. *Org. Mass Spectrom.* **1992**, *27*, 843.
(7) Danis, P. O.; Karr, D. E. *Org. Mass Spectrom.* **1993**, *28*, 923−925.

(8) Bahr, U.; Deppe, A.; Karas, M.; Hillenkamp, F. *Anal. Chem.* **1992**, *64*, 2866−2869.
(9) Montaudo, G.; Puglisi, C.; Samperi, F. *Macromolecules* **1995**, *28*, 4562−4569.
(10) Pasch, H.; Gores, F. *Polymer* **1995**, *36*, 1999−2005.
(11) Pasch, H.; Zammert, I. *J. Liq. Chromatogr.* **1994**, *17*, 3091−3108.
(12) Danis, P. O.; Karr, D. E.; Simonsick, W. J., Jr.; Wu, D. T. *Macromolecules* **1995**, *28*, 1229−1232.
(13) Danis, P. O.; Karr, D. E. *Macromolecules* **1995**, *28*, 8548−8551.
(14) Lehrle, R. S.; Sarson, D. S. *Rapid Commun. Mass Spectrom.* **1995**, *9*, 91−92.
(15) Dr. Andrew Bowdler, private communications, Kratos Analytical, Barton Dock Rd., Urmston, Manchester M41 7LD, UK.
(16) Haddleton, D. M.; Mahoney, D. R.; Sudderby, K. G. accepted for publication in *Macromolecules*.
(17) SEC calibrated for PMMA was employed to characterize the PEG sample giving $M_n = 2174$, $M_w = 2251$, and $PD_i = 1.035$. Due to the SEC calibration procedure used, large systematic deviations are expected in the molecular weights determined for PEG samples.
(18) Strupat, K.; Karas, M.; Hillenkamp, F. *Int. J. Mass Spectrom. Ion Proc.* **1991**, *111*, 89.
(19) Westman, A.; Demirev, P.; Huth-Fehre, T.; Bielawski, J.; Sundqvist, B. U. R. *Int. J. Mass Spectrom. Ion Proc.* **1994**, *130*, 107−115.
(20) Dey, M.; Grotemeyer, J. *Eur. Mass Spectrom.* **1995**, *1*, 95−103.
(21) Dey, M.; Castoro, J. A.; Wilkins, C. L. *Anal. Chem.* **1995**, *67*, 1575−1579.
(22) Perera, I. K.; Allwood, D.; Dyer, P. E.; Oldershaw, G. A *Int. J. Mass Spectrom. Ion Proc.* **1995**, *145*, L9−L16.
(23) Ens, W.; Mao, Y.; Standing, K. G. *Rapid Commun. Mass Spectrom.* **1991**, *5*, 117−123.
(24) Bökelmann, V.; Spengler, B.; Kaufmann, R. *Eur. Mass Spectrom.* **1995**, *1*, 81−93.
(25) Chaurand, P.; Della Negra, S.; Deprun, C.; Hoyes, J.; Le Beyec Y.; Aksouh, F. Book of Abstracts, 42nd ASMS Conference on Mass Spectrometry and Allied Topics, May 29−June 3, 1994, Chicago, IL.
(26) Spengler, B.; Bökelmann, V. *Nucl. Instrum. Meth. Phys. Res. B* **1993**, *82*, 379−385.
(27) Mowat, I. A.; Donovan, R. J.; Maier, R. M. Presented at the British Mass Spectrometry Society 21st Annual Meeting, Sept 3−6, 1995, Manchester, UK.
(28) Geno, P. W.; Macfarlane, R. D. *Int. J. Mass Spectrom. Ion Proc.* **1989**, *92*, 195−210.
(29) Axelsson, J.; Parilis, E. S.; Reimann, C. T.; Sullivan, P.; Sundqvist, B. U. R. *Nucl. Instrum. Meth. Phys. Res. B* **1995**, *101*, 343−356.
(30) Improved Detection of Polydispersed Polymers by Combining MALDI-TOF MS with SEC Fractionation. Hoberg, Anne-Mette; Haddleton, David M.; Scrivens, Jim H.; Derrick, Peter J.; Book of Abstracts, 44th ASMS Conference on Mass Spectrometry and Allied Topics, Portland, OR, May 12−16, 1996.

MA960350Z